ELSEVIER

Journal of Molecular Structure (Theochem) 461–462 (1999) 29–40

THEO CHEM

Mechanism of the oxidation of acetylene on a Ag surface: dipped adcluster model study ☆

Zhen-Ming Hu[a,d], Hiroyuki Ito[a], Seiichi Hara[a], Hiroshi Nakatsuji[a,b,c,*]

[a] *Department of Synthetic Chemistry and Biological Chemistry, Graduate School of Engineering, Kyoto University, Sakyo-ku, Kyoto 606, Japan*
[b] *Department of Applied Chemistry, Graduate School of Engineering, The University of Tokyo, Hongo, Tokyo 113, Japan*
[c] *Institute for Fundamental Chemistry, 34-4 Takano-Nishihiraki-cho, Sakyo-ku, Kyoto 606, Japan*
[d] *Department of Chemistry, Hubei Normal University, Huangshi 435002, P.R. China*

Received 25 May 1998; accepted 2 July 1998

Abstract

The mechanism of the oxidation of acetylene on a silver surface was studied by the dipped adcluster model (DAM) combined with ab initio Hartree–Fock and MP2 calculations. The reactions of the hydrogen and carbon of acetylene with both molecularly and atomically adsorbed oxygens were investigated. Our results show that the reaction path for acetylene via epoxidation is energetically unfavorable. On the other hand, the reaction path via hydrogen abstraction is much easier and leads to surface acetylide and hydroxyl intermediates, and is likely the initial reaction path responsible for the complete oxidation reaction of acetylene on a silver surface. The reaction mechanisms derived adequately explain the available experimental results.

Keywords: Silver surface; Acetylene; Oxidation reaction mechanism; Dipped adcluster model (DAM); Ab initio HF and MP2 methods

1. Introduction

The heterogeneous selective oxidation of hydrocarbons is an area of immense industrial importance, and has been the subject of extensive studies [1–38]. Most such studies are carried out on a silver surface, since silver is a uniquely effective catalyst for the epoxidation of ethylene to ethylene oxide in a practical industrial setting. Current research is focused on the fundamental reaction mechanisms, to understand the mechanistic details of the surface oxidation reaction and to identify a more effective catalyst for epoxide formation.

☆ Dedicated to Professor Keiji Morokuma in celebration of his 65th birthday.

* Corresponding author. Tel.: +81 75 7535653; fax: +81 75 7535910; e-mail: hiroshi@sbchem.kyoto-u.ac.jp

0166-1280/99/$ - see front matter
PII: S0166-1280(98)00463-1

For the epoxidation of ethylene, two mechanisms involving surface molecular oxygen [8–18] and atomic oxygen [22–31] as the active species have been suggested. The unique catalytic activity of silver has been the subject of long-standing interest, since other metal surfaces such as copper and gold are not good catalysts for this reaction [1–7]. On the other hand, excluding ethylene, only a few olefins such as styrene [33,34], 3,3-dimethylbutene [35], norbornene [36] and butadiene can be epoxidized on a silver surface. Other olefins, such as propylene [8–14], butenes [14] and pentenes [14], are mainly combusted into CO_2 and H_2O. Thus, there appear to be two main factors which determine the reaction mechanism of the surface oxidation of hydrocarbons: i.e. the metal used and the structure specificity of the hydrocarbon itself.

To clarify the mechanistic details of the oxidation of hydrocarbons on a silver surface, we previously studied the epoxidation and complete oxidation of ethylene [39,40] and propylene [41,42] on a silver surface by the dipped adcluster model (DAM) [43–45] combined with ab initio molecular orbital methods. Our theoretical studies showed that the uniquely high reactivity of a silver surface for ethylene epoxidation is due to its ability to adsorb an oxygen molecule as the end-on superoxide species [39]. Such a superoxide species cannot exist on the surface of copper or gold [46]. A higher selectivity of ethylene epoxidation is possible if the selectivity from ethylene to ethylene oxide by atomically adsorbed oxygen can be increased [40]. The low selectivity of propylene epoxidation is due to the presence of an allylic hydrogen, which shows higher reactivity toward the adsorbed oxygen than the olefinic carbon atom, leading to the formation of surface hydroxyl and allyl species [41]. In this case, the complete oxidation reaction is preferred. Based on our theoretical results, the general mechanism of the oxidation reaction of olefins on a silver surface is as follows: olefins which contain no allylic hydrogen and/or no subsequent resonance-stabilized allyl radical or anion formation mainly lead to epoxidation, while those which contain allylic hydrogen mainly lead to complete oxidation. Thus, whether epoxidation or complete oxidation occurs on a silver surface is determined by the reactivity of the olefinic carbon atoms and the allylic hydrogen of the olefins.

In this report, we extend our study to the oxidation of an alkyne on a silver surface. In contrast to olefins, experimental studies have shown that alkynes such as acetylene [37] and propyne [38] only undergo complete oxidation; no epoxidation products have been reported on a silver surface. In this report, we focus on acetylene as an example. We study the mechanisms of the reaction of acetylene with adsorbed oxygen on a silver surface, and seek to clarify why only complete oxidation, and not epoxidation, occurs.

2. Computational details

The theoretical methods used in the present study are the same as those used previously [39–42], i.e. the dipped adcluster model (DAM) [43–45] combined with ab initio HF and MP2 calculations. The DAM [43] was proposed as a theoretical model to study chemisorptions and surface reactions involving electron transfer between bulk metal and admolecules. Our previous studies have shown that electron transfer, electrostatic interaction (image force), and electron correlations are very important for the chemisorption of oxygen [47,48] and the oxidation reactions of olefins [39–42] on a silver surface.

Since acetylene is not adsorbed on a clean silver surface [37], like ethylene, the Eley–Rideal mode, which corresponds to the reaction between gaseous acetylene and the adsorbed oxygen species, is used in the present study. The activities of the C–H and C–C bonds of acetylene are studied by examining its reactivity with both molecularly adsorbed superoxide and atomically adsorbed oxygen on a silver surface. The model used was the same as that in previous studies [39–42]. Electron exchange between the adcluster and the bulk metal is taken into account by the DAM. Since we use the highest spin coupling model [43], one electron is transferred ($n = 1$) from a bulk metal into the adcluster, as shown previously [39–42]. The electrostatic interaction between the admolecule and the extended surface is estimated by the image force correction [44].

The geometries of the reactants, products, intermediates, and transition states (TSs) are optimized by the energy gradient method at the HF level, except for the Ag–Ag distance and the Ag_b–Ag_a–O_a angle which were fixed at 2.8894 Å and 90.0°, respectively. The electron correlations are considered by the MP2 method. In all cases, energy is expressed in kcal/mol, and bond distances and angles are in angstroms and degrees, respectively. The calculations were performed using the Gaussian94 software package [49].

The Gaussian basis set for the silver atom was (3s3p4d)/[3s2p2d] and the Kr core was replaced by the relativistic effective core potential [50]. For oxygen, we used the (9s5p)/[4s2p] set of Huzinaga–Dunning [51,52] augmented by diffuse s and p functions of $\alpha = 0.059$ as anion bases [53]. Polarization d functions of $\alpha = 2.704$, 0.535 [54] were added to the oxygen basis in the MP2 calculations. For carbon and hydrogen, the (9s5p)/[4s2p] and (4s)/[2s] sets, respectively, of Huzinaga–Dunning were used [51,52]. The validity of the present basis functions as well as the effect of electron corrections have been demonstrated in the previous studies [39].

3. Results and discussion

It is well known that several adsorbed oxygen species exist on a silver surface. To study the oxidation of hydrocarbons on a silver surface, it is necessary to consider the reaction with both molecularly and atomically adsorbed oxygen species. Our previous studies have shown that the active species for the epoxidation of ethylene on a silver surface is the molecularly adsorbed superoxide O_2^- [39]. The outside oxygen is more reactive, while the inner oxygen is more negative [47,48]. Atomically absorbed oxygen, which is left after the epoxidation, is active for both epoxidation and complete oxidation [39]. For propylene, both the superoxide and atomic oxygen species lead to complete oxidation [41]. While the reason for the complete oxidation of alkyne on a silver surface is unclear, we suppose that the main reaction mechanism is similar to that of olefins, i.e. differences may be due to the different reactivities of hydrogen and carbon in alkynes. In the case of acetylene, since there is only one kind of hydrogen and carbon, the reaction paths of the carbon and hydrogen with molecularly or atomically adsorbed oxygen would be illustrated as in Fig. 1.

3.1. Reaction of carbon with the adsorbed superoxide species

In this section, we study the reactivity of the carbon of acetylene with the molecularly adsorbed superoxide species. The reaction path is shown in Fig. 1a. As shown previously [39,47], the active species of the molecularly adsorbed oxygen is the superoxide O_2^-. When carbon attacks the superoxide species on the surface, it attacks the terminal oxygen, since it is more reactive than the inner oxygen. Fig. 2 shows the energy diagram for this reaction path. The energy is given relative to the free system, Ag_2 plus O_2 plus C_2H_2. An in-plane reaction pathway is used, i.e. the $Ag_2O_2C_2H_2$ adcluster is kept in the same plane and maintains C_s symmetry throughout the reaction, since it has been previously shown to be the most favorable pathway [39–42]. Starting from the oxygen adsorption state, we examined each reaction step in detail by optimizing the geometries of the intermediates and the transition states (TSs) along the reaction pathway.

When the carbon of acetylene attacks the terminal oxygen, O_b, a transition state (TS1) with an activation energy of 4.8 kcal/mol is obtained. The energy level of the intermediate is 28 kcal/mol, which is similar to that of the superoxide adsorption state (26.9 kcal/mol). In the TS the C–C bond distance increases from 1.20 Å in gaseous acetylene to 1.30 Å, and the O–O distance increases from 1.39 Å in the adsorption state to 1.48 Å. The C_a–O_b distance is calculated to be 1.82 Å. These changes indicate that the O–O and C–C bonds are weakened in the TS, and the C_a–O_b σ-bond begins to be formed. After the TS, we obtain an intermediate with a C–C distance of 1.35 Å, a C_a–O_b distance of 1.37 Å and an O–O distance of 1.49 Å. At this stage, the C_a–O_b σ-bond is complete, and the triple C≡C bond changes to a double C=C bond.

Table 1 shows the net charge and the frontier

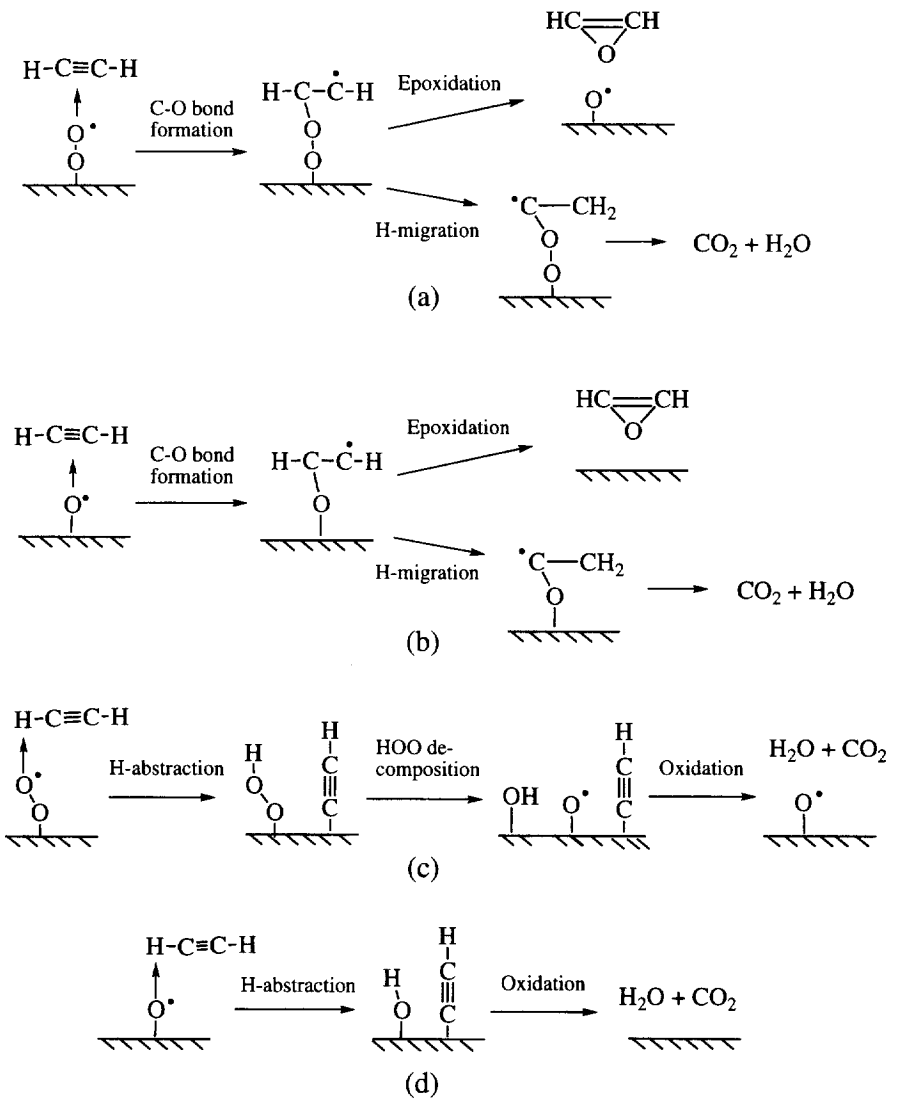

Fig. 1. Proposed reaction paths for the reaction of acetylene with adsorbed oxygen on a silver surface. (a) Reaction path of carbon with molecularly adsorbed superoxide. (b) Reaction path of carbon with atomically adsorbed oxygen. (c) Reaction path of hydrogen with molecularly adsorbed superoxide. (d) Reaction path of hydrogen with atomically adsorbed oxygen.

density (spin population) of the $Ag_2O_2C_2H_2$ adcluster along the reaction path shown in Fig. 2. Changes in the net charge and frontier density are mainly seen for the O_a, O_b, C_a, and C_b atoms, which represent the reaction center of the system. In the oxygen adsorption state, the frontier density of the terminal O_b is 0.784, which is larger than that of O_a (0.203). On the other hand, in the intermediate state, the largest frontier density of 1.01 is situated on the terminal C_b atom. Thus, since the frontier density reflects the reactivity of the atom, the reactive site shifts from O_b in the adsorbed oxygen state to C_b in the intermediate state.

When the intermediate is formed, two possible reaction paths exist for subsequent reactions. In one, the reactive site C_b attacks O_b, which may lead to cleavage of the O–O bond and formation

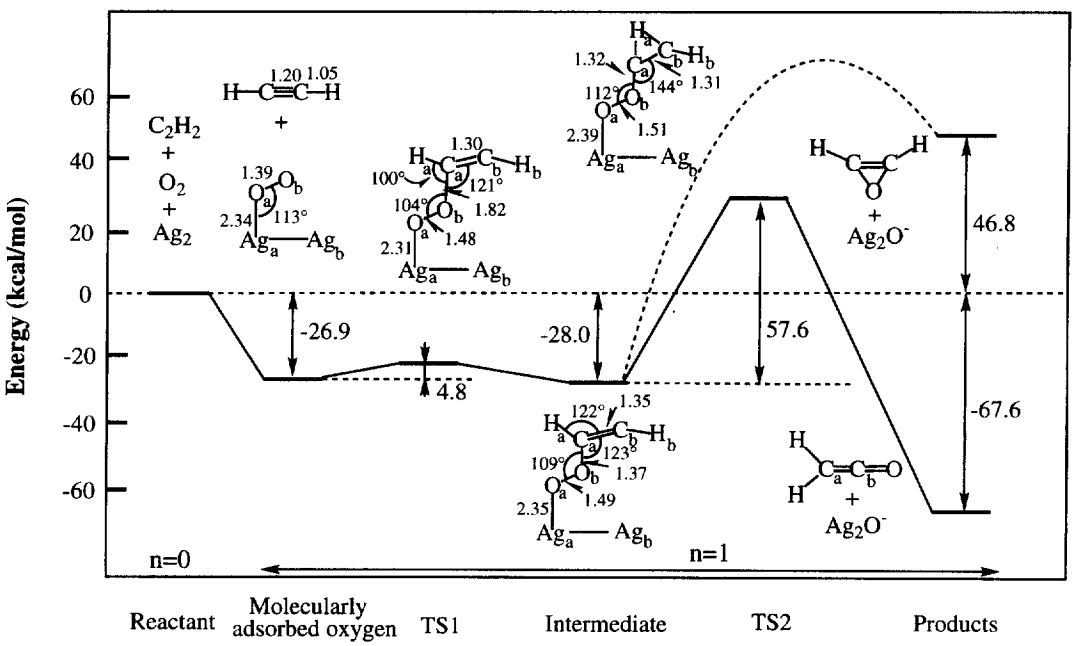

Fig. 2. Energy diagram for the reaction between carbon and molecularly adsorbed oxygen on a Ag surface. The routes leading to acetylene oxide and ketene are shown by broken and solid lines, respectively.

Table 1
Net charge and frontier density calculated by MP2 method for the Ag_2O_2–C_2H_2 adcluster shown in Fig. 2

	Adsorbed oxygen	TS for appro.	Intermediate dissoc.	TS for H mig	TS acet. oxi.	Product ketene	Product
Net charge							
Ag_a	−0.028	−0.059	−0.032	−0.006	−0.031	−0.058	−0.058
Ag_b	−0.197	−0.232	−0.246	−0.270	−0.234	−0.300	−0.300
O_a	−0.558	−0.624	−0.646	−0.568	−0.627	−0.642	−0.642
O_b	−0.217	−0.210	−0.248	−0.345	−0.205	−0.483	−0.353
C_a	−0.244	+0.102	+0.274	+0.263	+0.244	−0.055	−0.720
C_b	−0.244	−0.428	−0.501	−0.487	−0.594	−0.055	+0.581
H_a	+0.244	+0.230	+0.204	+0.226	+0.250	+0.296	+0.246
H_b	+0.244	+0.219	+0.195	+0.187	+0.197	+0.296	+0.246
Frontier density							
Ag_a	+0.182	+0.496	−0.035	+0.366	−0.467	−0.108	−0.108
Ag_b	−0.169	−0.514	+0.040	−0.371	+0.501	+0.077	+0.077
O_a	+0.203	+0.497	−0.067	−0.245	−0.051	+1.031	+1.031
O_b	+0.784	+0.059	+0.043	+0.244	+0.075	0.0	0.0
C_a	0.0	−0.362	−0.016	−0.072	+0.511	0.0	0.0
C_b	0.0	+0.808	+1.011	+1.049	+0.375	0.0	0.0
H_a	0.0	+0.026	+0.009	+0.018	−0.035	0.0	0.0
H_b	0.0	−0.011	+0.016	+0.011	+0.092	0.0	0.0

of acetylene oxide. The other path involves the migration of H_a from C_a to C_b, which would lead to the formation of a ketene. When the ketene is formed, it will prefer further combustion in the presence of adsorbed oxygen [55]. The resulting atomically adsorbed oxygen on the silver surface also reacts with acetylene, as shown in Fig. 1b. Fig. 2 shows that the product of acetylene oxide $+ Ag_2O^-$ is 46.8 kcal/mol more unstable than the free system, and 74.8 kcal/mol more unstable than the intermediate. This result shows that the reaction path for acetylene oxide formation is energetically unfavorable, and the epoxidation of acetylene does not occur on a silver surface, which is totally different from previous results with olefins on the same silver surface [39–42]. Although the product of ketene $+ Ag_2O^-$ is about 40 kcal/mol more stable than the intermediate, the energy barrier for H_a migration is calculated to be 57.6 kcal/mol. This reaction path is also unfavorable compared with that described below, in which hydrogen reacts with the superoxide species. Experimentally, no epoxidation product or ketene has been identified in the reaction of acetylene with adsorbed oxygen on a silver surface [37].

3.2. Reaction of hydrogen with the adsorbed superoxide species

Fig. 1c shows the reaction path for the reaction of the hydrogen of acetylene with the superoxide species on a silver surface. This reaction path consists of two steps: hydrogen abstraction and HO–O decomposition. In the first step, one hydrogen of acetylene is abstracted by the terminal oxygen of the superoxide, leading to the adsorbed hydroperoxyl species (HOO(a)) and the adsorbed acetylide species (C_2H(a)). The next step is the decomposition of the adsorbed hydroperoxyl group to the adsorbed surface hydroxyl group (HO(a)) and the adsorbed atomic oxygen (O(a)), as shown in a former study on the oxidation of propylene [41]. Two surface hydroxyl groups can be disproportionated to produce water and one adsorbed oxygen on a silver surface [28,29,56]. The adsorbed oxygen atom produced in this process is reactive in further oxidation, as shown in Fig. 1d. The adsorbed acetylide species should be readily oxidized to CO_2 and H_2O in the presence of adsorbed oxygens, as shown experimentally [37].

Fig. 3 shows the fully optimized geometries and the energy diagram for the hydrogen abstraction reaction step. When hydrogen approaches the superoxide species, an intermediate state with a stabilization energy of 11.4 kcal/mol is obtained. At this stage, the geometry of acetylene is almost the same as that of the free gaseous species. The process leading to the TS includes the formation of a weak σ-bond between the hydrogen and the terminal oxygen atom (O_b). The H_a–O_b distance is 1.40 Å and the C_a–H_a distance is 1.19 Å, which is comparable to 1.06 Å in the free acetylene molecule. The O_a–O_b distance also increases from 1.39 Å in the adsorbed superoxide state to 1.42 Å. The carbon of acetylene seems to interact with the surface, although the C–Ag distance is as large as 2.6 Å. The C–C distance is 1.22 Å, which is comparable to 1.20 Å in the free acetylene molecule. The net charge and frontier density of this reaction step are shown in Table 2.

The energy barrier in this step was calculated to be 12.5 kcal/mol, which is much smaller than that of the reaction paths leading to the formation of acetylene oxide and a ketene shown in Fig. 2. The energy level of the coadsorbed OOH and C_2H state was calculated to be stable by 57.6 kcal/mol, and further stabilization of 42.6 kcal/mol is achieved in the subsequent OOH decomposition step [41]. Compared with the results shown in Fig. 2, the pathway via hydrogen abstraction shown in Fig. 3 is much easier, and should be the initial reaction step leading to the complete oxidation of acetylene on a silver surface.

3.3. Reactions with atomically adsorbed oxygen

We investigated the energetics and pathways of the reactions of carbon and hydrogen with atomically adsorbed oxygen on a Ag surface. Atomically adsorbed oxygen on a Ag surface is produced through the peroxide species of molecularly adsorbed oxygen [39,48]. As shown in Fig. 2, it is also a product of the oxidation reaction of

Table 2
Net charge and frontier density calculated by MP2 method for the Ag_2O_2–C_2H_2 adcluster shown in Fig. 3

	Adsorbed oxygen	Intermediate state	Transition	Intermediate
Net charge				
Ag_a	−0.028	+0.007	−0.191	+0.003
Ag_b	−0.197	−0.190	−0.169	+0.246
O_a	−0.588	−0.443	−0.170	−0.547
O_b	−0.217	−0.366	−0.462	−0.644
C_a	−0.244	−0.132	−0.022	−0.162
C_b	−0.244	−0.461	−0.491	−0.563
H_a	+0.244	+0.343	+0.263	+0.458
H_b	+0.244	+0.242	+0.242	+0.207
Frontier density				
Ag_a	+0.182	+0.004	−0.032	+0.424
Ag_b	−0.169	+0.008	+0.022	+0.507
O_a	+0.203	+0.350	+0.869	+0.015
O_b	+0.784	+0.634	+0.149	+0.002
C_a	0.0	+0.021	+0.003	+0.203
C_b	0.0	−0.017	+0.011	−0.166
H_a	0.0	−0.002	−0.024	−0.000
H_b	0.0	+0.001	+0.002	+0.015

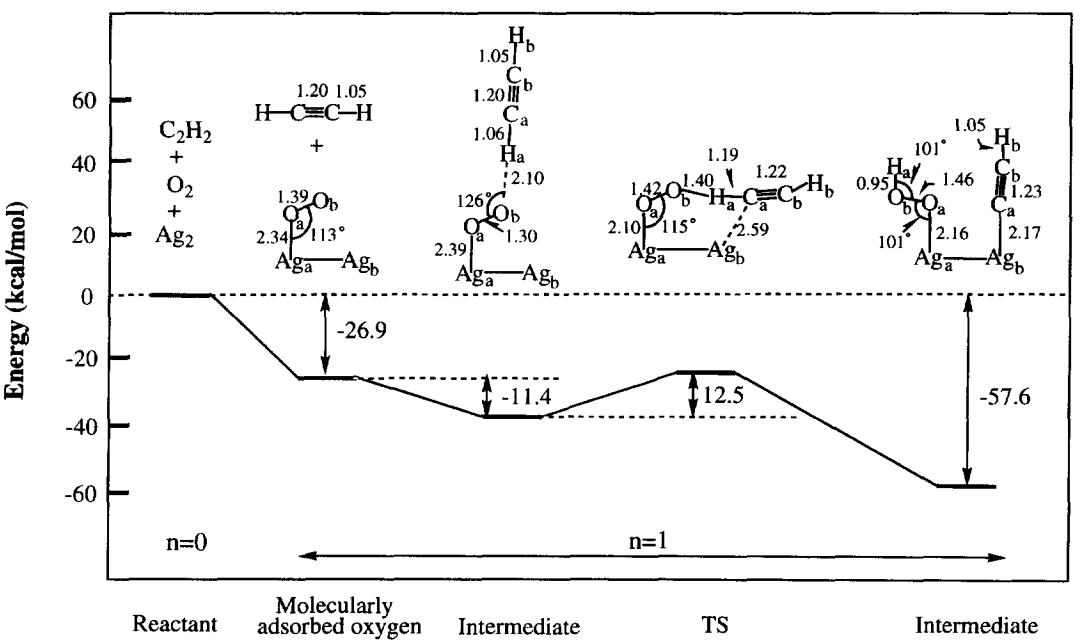

Fig. 3. Energy diagram for the reaction between hydrogen and molecularly adsorbed oxygen on a Ag surface.

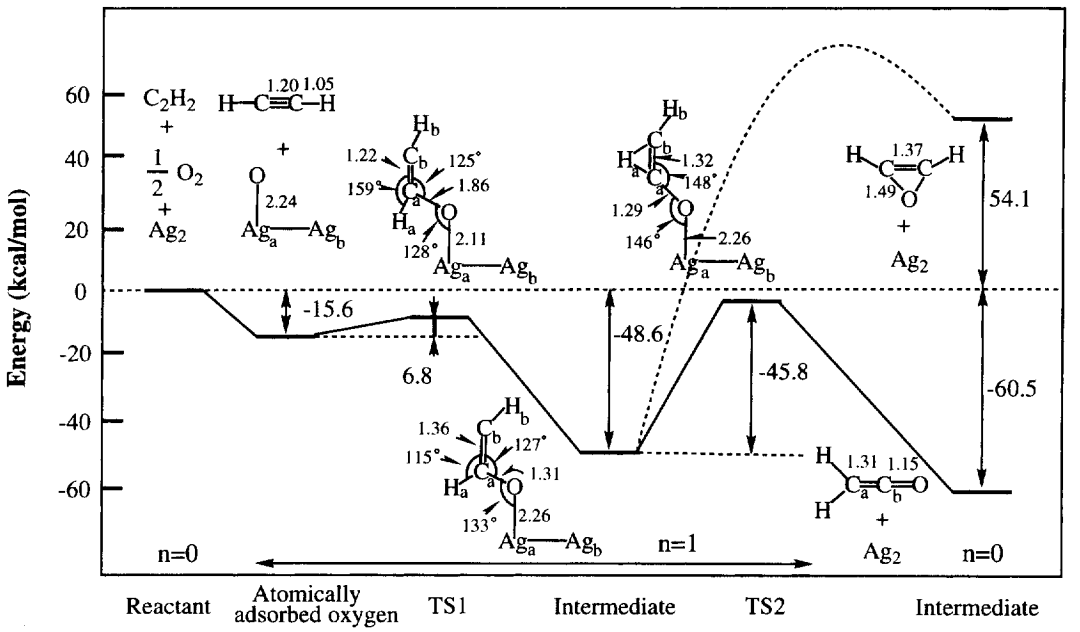

Fig. 4. Energy diagram for the reaction between carbon and atomically adsorbed oxygen on a Ag surface. The routes leading to acetylene oxide and ketene are shown by broken and solid lines, respectively.

acetylene with the molecularly adsorbed superoxide species. The net charge and frontier density of the atomically adsorbed oxygen on the silver surface are calculated to be −0.642 and +1.031, respectively. This spin population exists on the in-plane $2P_x$ orbital, which is parallel to the Ag–Ag bond. An in-plane reaction pathway with C_s symmetry is then adopted, as shown in Fig. 1b and d.

Fig. 1b shows the reaction path of carbon with

Table 3
Net charge and frontier density calculated by MP2 method for the Ag_2O–C_2H_2 adcluster shown in Fig. 4

	Adsorbed oxygen	TS for appro.	Intermediate	TS for dissoc.	Product
Net charge					
Ag_a	−0.058	−0.129	−0.122	−0.131	0.0
Ag_b	+0.300	−0.259	−0.241	−0.234	0.0
O	−0.642	−0.559	−0.592	−0.504	−0.353
C_a	−0.244	−0.048	+0.241	+0.154	−0.720
C_b	−0.244	−0.415	−0.579	−0.628	+0.581
H_a	+0.244	+0.191	+0.113	+0.169	+0.246
H_b	+0.244	+0.219	+0.180	+0.175	+0.246
Frontier density					
Ag_a	−0.108	−0.370	−0.033	−0.018	0.0
Ag_b	+0.077	+0.392	+0.021	+0.035	0.0
O	+1.031	+0.740	−0.029	+0.127	0.0
C_a	0.0	−0.460	−0.052	+0.433	0.0
C_b	0.0	+0.676	+0.938	+0.289	0.0
H_a	0.0	+0.026	−0.009	+0.014	0.0
H_b	0.0	−0.004	+0.030	+0.120	0.0

atomically adsorbed oxygen. When carbon attacks atomically adsorbed oxygen on the surface, the most favorable approach is the formation of a C–O bond. Fig. 4 shows the geometries and the energy diagram in this reaction path. The net charge and frontier density of the adcluster in each reaction step are shown in Table 3. The energy barrier from the adsorbed oxygen to the intermediate is calculated to be 6.8 kcal/mol. The C–O distances in the TS and the intermediate are calculated to be 1.86 and 1.31 Å, respectively. The C–C bond distance increases from 1.20 Å in the reactant to 1.22 Å in the TS, and further to 1.36 Å in the intermediate: it changes from a triple bond to a double bond. Although the intermediate is much more stable than the free system, the total energy diagram is similar to that given above for the reaction with molecularly adsorbed superoxide species, i.e. formation of the acetylene oxide is energetically impossible and the energy barrier leading to ketene formation is high.

Fig. 1d shows the reaction path of hydrogen with atomically adsorbed oxygen on a silver surface. The energy diagram for this reaction path is shown in Fig. 5, and the net charge and the spin population are shown in Table 4. The hydrogen of acetylene approaches the atomically adsorbed oxygen to give an intermediate that is 8.7 kcal/mol more stable than the adsorbed oxygen state. The structure of acetylene in this state is almost the same as that of gaseous acetylene, and the O–H_a bond is as long as 1.94 Å. The electronic structure of this state is not much different from that of the adsorbed oxygen state.

When hydrogen further approaches the adsorbed oxygen, the subsequent reaction occurs rapidly, leaving the adsorbed OH and acetylide on the Ag surface: the energy barrier of this process is only 6 kcal/mol. The heat of reaction was calculated to be 73.6 kcal/mol. In this process, the O–H_a distance decreases from 1.94 Å to 1.09 Å, and then to 0.95 Å, and the C_a–H_a distance increases from 1.08 to 1.55, and then to infinite. A reaction path which includes hydrogen abstraction from C_a–H_a to O–H_a is clear.

By comparing the energy diagrams in Fig. 4 and Fig. 5, it is clear that the reaction path via hydrogen abstraction by the adsorbed oxygen is definitely more favorable. The reaction of acetylene

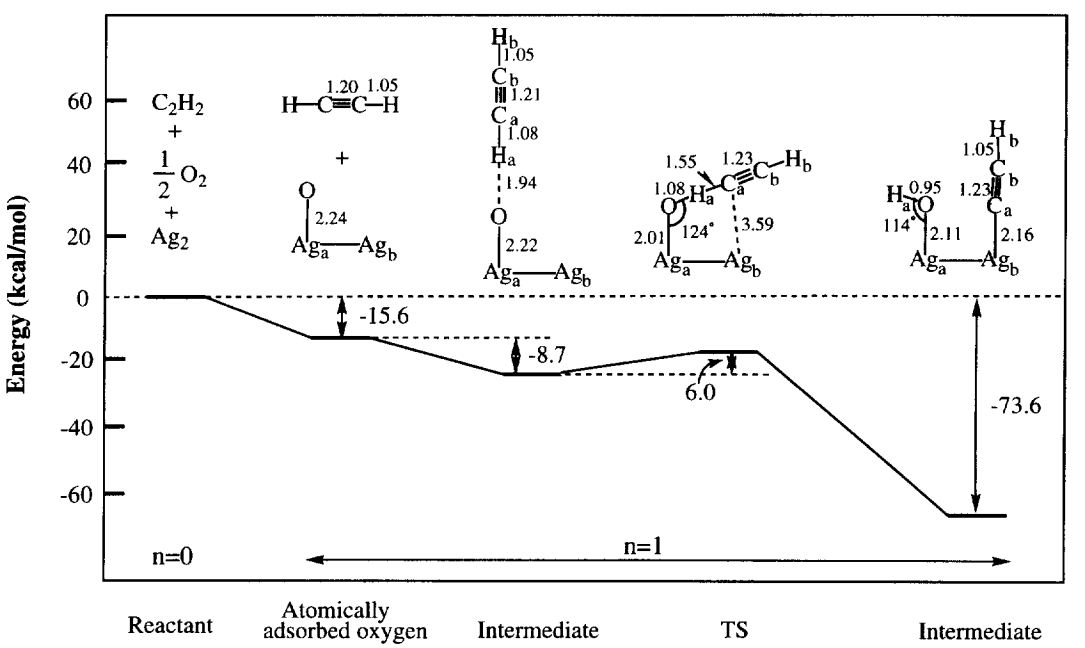

Fig. 5. Energy diagram for the reaction between hydrogen and atomically adsorbed oxygen on a Ag surface.

Table 4
Net charge and frontier density calculated by MP2 method for the $Ag_2O-C_2H_2$ adcluster shown in Fig. 5

	Adsorbed oxygen	Intermediate	Transition state	Intermediate
Net charge				
Ag_a	−0.058	−0.099	+0.001	+0.242
Ag_b	+0.300	−0.283	−0.102	−0.015
O	−0.642	−0.596	−0.726	−1.149
C_a	−0.244	−0.154	−0.196	−0.125
C_b	−0.244	−0.425	−0.571	−0.571
H_a	+0.244	+0.332	+0.403	+0.415
H_b	+0.244	+0.224	+0.191	+0.205
Frontier density				
Ag_a	−0.108	−0.123	−0.242	+0.454
Ag_b	+0.077	+0.095	+0.524	+0.447
O	+1.031	+1.032	+0.741	+0.043
C_a	0.0	+0.143	+0.441	+0.308
C_b	0.0	−0.142	−0.468	−0.274
H_a	0.0	−0.018	−0.039	−0.003
H_b	0.0	0.013	+0.043	+0.025

with atomically adsorbed oxygen on a silver surface leads to complete oxidation by the abstraction of hydrogen as the initial fundamental reaction step, which is the same result as when acetylene reacts with molecularly adsorbed superoxide on a silver surface. Our results show that the reactivity of the hydrogen of acetylene is higher than that of the carbon for oxygen adsorbed on a silver surface, and the initial fundamental reaction step can be summarized as:

$$H-C\equiv C-H + O_2/Ag \rightarrow H-C\equiv C/Ag + H-O-O/Ag \quad (1)$$

$$\rightarrow H-C\equiv C/Ag + H-O/Ag + O/Ag \quad (2)$$

$$H-C\equiv C-H + O/Ag \rightarrow H-C\equiv C/Ag + H-O/Ag \quad (3)$$

Barteau and Madix [37] studied the reaction of acetylene with oxygen on a Ag(110) surface. A surface acetylide species was suggested by thermal desorption and LEED experiments, and an acetylide intermediate was further confirmed by titration reactions: $HC_2(a)$ reacts with CH_3COOD to give HC≡CD [37]. An experiment with propyne [38] also showed that hydrogen abstraction and surface methyl acetylide formation is the main reaction step. These experimental findings support the reaction mechanisms shown in Eqs. (1)–(3). Although the reaction mechanism presented here is based only on a study of the oxidation of acetylene, it may reflect the general reaction mechanism for the oxidation of alkynes on a silver surface.

4. Conclusions

In this study, we examined the reaction mechanisms of the oxidation of acetylene on a silver surface by the dipped adcluster model (DAM) combined with the ab initio Hartree–Fock and MP2 methods. The reactivity of the hydrogen and the carbon of acetylene with both molecularly adsorbed superoxide and atomically adsorbed oxygen on a silver surface were examined, and the energy diagrams for the reaction paths leading to epoxidation and complete oxidation products are presented.

The reactions of acetylene with molecularly

and atomically adsorbed oxygen lead to the same results. Since the energy level of the acetylene oxide is very high compared with that of the free species, the formation of the epoxidation products is energetically impossible, which explains the experimental finding that no acetylene epoxidation products have been found on a silver surface.

The reactivity of the hydrogen of acetylene is higher than that of the carbon for surface oxidation reactions. The reaction paths via hydrogen abstraction lead to the formation of surface acetylide and hydroxyl species, which is the initial fundamental reaction step leading to the complete oxidation of acetylene on a silver surface. This reaction mechanism may also explain the oxidation of other alkynes on a silver surface.

The present results regarding the mechanism of acetylene oxidation combined with the results reported previously [39–42] give us a good understanding of the oxidation of olefins and alkynes on a silver surface. The DAM is essential for clarifying these kinds of surface oxidation mechanisms.

Acknowledgements

Some calculations were performed using the computers at the Institute for Molecular Science. Part of this study was supported by a Grant-in-Aid for Scientific Research from the Ministry of Education, Science, and Culture of Japan and by a grant from the Kyoto University VBL project.

References

[1] R.A. van Santen, H.P.C. Kuipers, Adv. Catal. 35 (1987) 265.
[2] W.M.H. Sachtler, C. Backx, R.A. van Santen, Catal. Rev. Sci. Eng. 23 (1981) 127.
[3] X.E. Verykios, F.P. Stein, R.W. Coughlin, Catal. Rev. Sci. Eng. 22 (1980) 197.
[4] K.A. Jørgensen, Chem. Rev. 89 (1989) 431.
[5] A. Ayame, Series of Lectures on Catalysis VII, Fundamental Industrial Catalytic Reaction; Catalytic Society of Japan, Y. Murakami, Tokyo, 1985, pp. 170–185, in Japanese.
[6] A. Ayame, H. Kanoh, Shokubai 20 (1978) 381, in Japanese.
[7] H. Miura, A. Ayame, H. Kanoh, K. Miyahara, I. Toyoshima, Shinku 25 (1982) 302.
[8] N.W. Cant, W.K. Hall, J. Catal. 52 (1978) 81.
[9] M. Imachi, M. Egashira, R.L. Kuczkowski, N.W. Cant, J. Catal. 70 (1981) 177.
[10] C. Henriques, M.F. Portela, C. Mazzocchia, E. Guglielminotti, in: L. Guczi et al. (Eds.), New Frontiers in Catalysis, 1993, pp. 1995–1998.
[11] M.F. Portela, C. Henriques, M.J. Pires, L. Ferreira, M. Baerna, Catal. Today 1 (1987) 101.
[12] P.V. Geenen, H.J. Boss, G.T. Pott, J. Catal. 77 (1982) 499.
[13] I.L.C. Freriks, R. Bouwman, P.V. Geenen, J. Catal. 65 (1980) 311.
[14] M. Akimoto, K. Ichikawa, E. Echigoya, J. Catal. 76 (1982) 333.
[15] C.T. Campbell, J. Catal. 94 (1985) 436.
[16] C.T. Campbell, J. Catal. 99 (1986) 28.
[17] C.T. Campbell, M.T. Paffett, Surf. Sci. 139 (1984) 396.
[18] C.T. Campbell, M.T. Paffett, Surf. Sci. 177 (1986) 417.
[19] J. Yang, J. Deng, X. Yuan, S. Zhang, Appl. Catal. A General 92 (1992) 731.
[20] J. Deng, J. Yang, S. Zhang, X. Yuan, J. Catal. 138 (1992) 395.
[21] Y. Peng, S. Zhang, L. Tang, J. Deng, Catal. Lett. 12 (1992) 307.
[22] E.L. Force, A.T. Bell, J. Catal. 38 (1975) 440.
[23] E.L. Force, A.T. Bell, J. Catal. 40 (1975) 356.
[24] R.B. Grant, R.M. Lambert, J. Catal. 92 (1985) 364.
[25] R.A. Van Santen, C.P.M. De Groot, J. Catal. 98 (1986) 530.
[26] J.T. Gleaves, A.G. Sault, R.J. Madix, J.R. Ebner, J. Catal. 121 (1990) 202.
[27] M.A. Barteau, R.J. Madix, J. Am. Chem. Soc. 105 (1983) 344.
[28] J.T. Roberts, R.J. Madix, W.W. Crew, J. Catal. 141 (1993) 300.
[29] E.A. Carter, W.A. Goddard, III, Surf. Sci. 209 (1989) 243.
[30] P.J. Van den Hoek, E.J. Baerends, R.A. Van Santen, J. Phys. Chem. 93 (1989) 6469.
[31] K.A. Jørgensen, R. Hoffmann, J. Phys. Chem. 94 (1990) 3046.
[32] S. Beran, P. Jiru, B. Wichterlova, R. Zahradnik, Proc. Sixth Int. Congr. Catal. 1 (1977) 324.
[33] Y. Murakomo, K. Tanaka, Nippon Kagaku Kaishi 11 (1977) 1603.
[34] S. Hawker, C. Mukoid, J.P.S. Badyal, R.M. Lambert, Surf. Sci. 219 (1989) L615.
[35] C. Mukoid, S. Hawker, J.P.S. Badyal, R.M. Lambert, Catal. Lett. 4 (1990) 57.
[36] J.T. Roberts, R.J. Madix, J. Am. Chem. Soc. 110 (1988) 8540.
[37] M.A. Barteau, R.J. Madix, Surf. Sci. 115 (1982) 355.
[38] J.M. Vohs, B.A. Carney, M.A. Barteau, J. Am. Chem. Soc. 107 (1985) 7841.
[39] H. Nakatsuji, H. Nakai, K. Ikeda, Y. Yamamoto, Surf. Sci. 384 (1997) 315.

[40] H. Nakatsuji, K. Takahashi, Z.M. Hu, Chem. Phys. Lett. 277 (1997) 551.
[41] Z.M. Hu, H. Nakai, H. Nakatsuji, Surf. Sci. 401 (1998) 371.
[42] H. Nakatsuji, Z.M. Hu, H. Nakai, Int. J. Quantum Chem. 65 (1997) 839.
[43] H. Nakatsuji, J. Chem. Phys. 87 (1987) 4995.
[44] H. Nakatsuji, H. Nakai, Y. Fukunishi, J. Chem. Phys. 95 (1991) 640.
[45] H. Nakatsuji, Proc. Surf. Sci. 54 (1997) 1.
[46] H. Nakatsuji, Z.M. Hu, H. Nakai, K. Ikeda, Surf. Sci. 387 (1997) 328.
[47] H. Nakatsuji, H. Nakai, Can. J. Chem. 70 (1992) 404.
[48] H. Nakatsuji, H. Nakai, J. Chem. Phys. 98 (1993) 2423.
[49] M.J. Frisch, G.W. Trucks, H.B. Schlegel, P.M.W. Gill, B.G. Johnson, M.A. Robb, J.R. Cheeseman, T.A. Keith, G.A. Petersson, J.A. Montgomery, K. Raghavachari, M.A. Al-Laham, V.G. Zakrzewski, J.V. Ortiz, J.B. Foresman, J. Cioslowski, B.B. Stefanov, A. Nanayakkara, M. Challacombe, C.Y. Peng, P.Y. Ayara, W. Chen, M.W. Wong, J.L. Andres, E.S. Replogle, R. Gomperts, R.L. Martin, D.J. Fox, J.S. Binkley, D.J. Defrees, J. Baker, J.P. Stewart, M. Head-Gordon, C. Gonzalez, J.A. Pople, Gaussian94 (Revision D.3), Gaussian, Inc., Pittsburgh, PA, 1995.
[50] P.J. Hay, W.R. Wadt, J. Chem. Phys. 82 (1985) 270.
[51] S. Huzinaga, J. Chem. Phys. 42 (1965) 1293.
[52] T.H. Dunning, Jr., J. Chem. Phys. 53 (1970) 2823.
[53] T.H. Dunning Jr., P.J. Hay, in: H.F. Schaeffer III (Ed.), Modern Theoretical Chemistry, vol. 3, Plenum, New York, 1977, p. 10.
[54] S. Huzinaga, J. Andzelm, M. Kiobukowski, E. Radzio-Anzelm, Y. Sakai, H. Tatewaki, Gaussian Basis Sets for Molecular Calculations, Physical Science Data vol. 16, Elsevier, Amsterdam, 1984, p. 23.
[55] L.Ya. Margolis, Adv. Catal. 14 (1963) 429.
[56] Z.M. Hu, H. Nakatsuji, in preparation.